






Article

# Room Temperature Mechanical Properties of A356 Alloy with Ni Additions from 0.5 Wt to 2 Wt %

Lucia Lattanzi <sup>1,\*</sup> , Maria Teresa Di Giovanni <sup>2</sup>, Maverick Giovagnoli <sup>1</sup> , Annalisa Fortini <sup>1</sup> ,  
Mattia Merlin <sup>1</sup> , Daniele Casari <sup>3</sup>, Marisa Di Sabatino <sup>4</sup>, Emanuela Cerri <sup>2</sup>  
and Gian Luca Garagnani <sup>1</sup> 

<sup>1</sup> Department of Engineering, University of Ferrara, Via G. Saragat 1, I-44122 Ferrara, Italy; maverick.giovagnoli@unife.it (M.G.); annalisa.fortini@unife.it (A.F.); mattia.merlin@unife.it (M.M.); gian.luca.garagnani@unife.it (G.L.G.)

<sup>2</sup> Department of Engineering and Architecture, University of Parma, Viale G. Usberti 18/A, I-43124 Parma, Italy; mariateresa.digiovanni@unipr.it (M.T.D.G.); emanuela.cerri@unipr.it (E.C.)

<sup>3</sup> Brembo SpA, Via G. M. Scotti 66, I-24030 Mapello (BG), Italy; Daniele\_Casari@brembo.it

<sup>4</sup> Department of Materials Science and Engineering, Norwegian University of Science and Technology, Alfred Getz vei 2 B, N-7491 Trondheim, Norway; marisa.di.sabatino.lundberg@ntnu.no

\* Correspondence: lucia.lattanzi@unife.it

Received: 6 February 2018; Accepted: 26 March 2018; Published: 29 March 2018



**Abstract:** In recent years, the influence of Ni on high-temperature mechanical properties of casting Al alloys has been extensively examined in the literature. In the present study, room temperature mechanical properties of an A356 alloy with Ni additions from 0.5 to 2 wt % were investigated. The role of Ni-based compounds and eutectic Si particles in reinforcing the Al matrix was studied with image analysis and was then related to tensile properties and microhardness. In the as-cast condition, the formation of the 3D network is not sufficient to determine an increase of mechanical properties of the alloys since fracture propagates by cleavage through eutectic Si particles and Ni aluminides or by the debonding of brittle phases from the aluminum matrix. After T6 heat treatment the increasing amount of Ni aluminides, due to further addition of Ni to the alloy, together with their brittle behavior, leads to a decrease of yield strength, ultimate tensile strength, and Vickers microhardness. Despite the fact that Ni addition up to 2 wt % hinders spheroidization of eutectic Si particles during T6 heat treatment, it also promotes the formation of a higher number of brittle Ni-based compounds that easily promote fracture propagation.

**Keywords:** casting al alloys; Ni addition; room temperature mechanical properties; microstructure

## 1. Introduction

Al-Si casting alloys are extensively used in automotive components in order to reduce both weight and fuel consumption. In this respect, in recent years a considerable amount of studies have concerned the improvement of their characteristics by melt inoculation [1], by the addition of alloying elements [2], and by the optimization of heat treatments and process parameters [3,4]. Since the mechanical properties of Al alloys rapidly decrease when the temperature increases, the addition of transition elements, such as Cu and/or Ni, is a key aspect for applications that require improved high-temperature resistance [5–8].

Differently from Cu, Ni has an extremely limited solubility in Al (0.05 wt % at 640 °C, i.e., the eutectic temperature, decreasing down to 0.003 wt % at 527 °C) and, thus, it is mainly found in intermetallic compounds with Al, Cu, or Fe. It has been proved that the presence of Ni in eutectic and hypoeutectic Al-Si alloys leads to the formation of thermally stable  $\epsilon$ -Al<sub>3</sub>Ni and T-Al<sub>9</sub>FeNi intermetallic compounds [9–11]. In particular, the latter one precipitates through a peritectic reaction from the

$\beta$ -Al<sub>5</sub>FeSi phase [12]. A Ni/Fe ratio of approximately 2 is considered the threshold, above which all the Fe present in the alloy is bound to Ni in the T-phase and the formation of the  $\beta$ -phase is suppressed [13]. These Ni-based aluminides and binary Al-Si eutectics are observed to nucleate in overlapping temperature ranges [14]. This leads to the formation of a three-dimensional (3D) interconnected network made of eutectic Si and Ni-based intermetallic phases. The interconnected structure acts as a rigid reinforcement for the aluminum matrix since both eutectic Si and Ni aluminides have higher strength and higher Young's modulus than primary Al [15]. In addition, it has been reported that the presence of Ni-bearing compounds has a poisoning effect on the spheroidization of Si eutectic particles during solution heat treatment. According to Asghar et al. [10], the interface between eutectic Si and Ni-based compounds is retained after solution heat treatment, and the reason for this phenomenon concerns the interfacial energy between aluminides and Si. This interfacial energy is more favorable than the one between primary Al and Si and, thus, stabilizes the interconnected structures of Si and Ni aluminides. These aluminides maintain the interconnection of the 3D network during eutectic Si spheroidization acting as linking elements for isolated Si particles. Therefore, the 3D network provides good high-temperature strength to the alloy and makes it suitable for applications that require high-temperature performances [10,16].

In previous studies, several authors evaluated the effect of Ni additions varying from 0.5 to 4 wt % [5,9,16–19] on near-eutectic Al-Si<sub>10</sub> and Al-Si<sub>12</sub> cast alloys, which are widely employed for cylinder heads and pistons. High-temperature compression strength is an important requirement for piston alloys since these components have to withstand severe compression stresses, as well as temperatures up to 400 °C during their service life [5,9]. Additionally, some authors investigated the influence of Ni on room-temperature mechanical properties [19,20]. Yang et al. [19] reported that the evolution of Ni-rich compounds has a beneficial effect on the room temperature mechanical properties of an Al-Si piston alloy; moreover, the elevated temperature tensile strength was observed to increase by about 19.7%. Yang et al. [20] found that the addition of Ni to an Al-Mg-Si-Mn alloy resulted in a slight increase in both room temperature yield strength and ultimate tensile strength.

Hypoeutectic Al-Si alloys, such as the A356 alloy, are the most used Al foundry alloys in several automotive applications, which require both room and high temperature services. Few authors [7,21–23] investigated the influence of Ni on tensile mechanical properties of hypoeutectic Al-Si alloys at both room- and high-temperature. These works report contradictory findings, and the actual influence of Ni on the mechanical properties is yet to be determined. Stadler et al. [21] investigated the effect of different Ni amounts (0.5, 1, and 1.5 wt %) on the high-temperature mechanical properties of T4 heat-treated specimens. Yield strength, ultimate tensile strength, and percentage elongation were found to increase up to 1 wt % of Ni. No further increase in mechanical properties was observed at higher Ni concentrations. Casari et al. [7] studied the effect of different Ni concentrations (0.5, 1, and 2 wt %) on high-temperature mechanical properties by comparison of as-cast and T6 heat-treated specimens. The authors reported that Ni contents over 0.5 wt % determine a significant reduction of both yield strength and ultimate tensile strength in heat-treated alloys. Fang et al. [22] reported that the Ni and Sr-containing A380 alloy exhibits a significant improvement in tensile properties, specifically ultimate tensile strength and yield strength. Garcia-Hinojosa et al. [23] examined the effect of Ni additions (0.5 and 1 wt %) on room temperature mechanical properties of as-cast A356 alloys, both unmodified and modified with Sr. In both alloys, Ni additions did not improve the mechanical properties compared to the base A356 alloy because of the presence of massive  $\epsilon$ -Al<sub>3</sub>Ni conglomerates that weaken the alloy structural characteristics.

Additionally, to the knowledge of the authors, there exist very few reports on the effect of Ni additions on room temperature mechanical properties of hypoeutectic Al-Si alloys in both as-cast and T6 conditions. For this reason, efforts were devoted to explore how the addition of Ni influences the evolution of microstructure and room temperature performances of hypoeutectic Al-Si alloys. A comprehensive investigation consisting of tensile and microhardness tests has been carried out to reveal the role played by Ni-based intermetallic compounds on the room temperature tensile properties

of the A356 aluminum casting alloy (AlSi7Mg0.3, belonging to the AlSi7Mg alloy group, i.e., UNI EN 42000) added with 0.5, 1, and 2 wt % of Ni in as-cast and T6 heat-treated conditions. Microstructural investigations, associated with statistical analysis of representative geometrical parameters of Ni-based compounds and eutectic Si particles, were carried out to describe possible variations of microstructural features with increased Ni additions. Furthermore, fractographic observations were performed to evaluate the role of Ni aluminides on the fracture behavior of the examined alloys.

## 2. Materials and Methods

### 2.1. Melt Preparation and Specimen Casting

A commercial purity A356 alloy was melted in a boron-nitride coated clay-graphite crucible and kept at 1013 K (740 °C). Ni was added to the melt from an Al-10 wt % Ni master alloy according to the targeted nominal concentrations of 0.5, 1, and 2 wt %, and held for 10 min to reach complete dissolution. Molten metals were then degassed with Ar gas for 10 min just prior to casting. Permanent mold castings were obtained by pouring the molten alloy into an L-shaped preheated steel mold manufactured according to the UNI EN 1706:2010 specification. Die temperature was kept at 573 K (300 °C) during all casting trials. Samples from the three different melts were taken and analyzed by glow discharge optical emission spectroscopy (GD-OES, Horiba Scientific, Palaiseau, Île-de-France, France). The chemical composition of the prepared alloys is given in Table 1. With the exception of the Ni contents, the concentration of each alloying element is in compliance with the UNI EN 1706:2010 specification for AlSi7Mg alloys.

**Table 1.** The chemical composition of the investigated alloys (wt %).

Alloy	Si	Fe	Mg	Ni	Al	Condition
A356 + 0.5 wt % Ni	6.64	0.08	0.24	0.44	balance	As-cast T6
A356 + 1 wt % Ni	6.87	0.08	0.25	0.95	balance	As-cast T6
A356 + 2 wt % Ni	7.13	0.08	0.23	1.88	balance	As-cast T6

The T6 heat treatment involved a two-step solution treatment carried out at 793 K (520 °C) for 2 h and then at 813 K (540 °C) for 2 h, quench in a water bath at 293 K (20 °C), and final aging at 433 K (160 °C) for 6 h [7].

### 2.2. Tensile and Microhardness Tests

Tensile specimens with a round cross-section (8.5 mm diameter and 40 mm gauge length) were machined and subsequently tested at room temperature with an MTS 810 servo-hydraulic testing machine (MTS Systems, Turin (TO), Italy) equipped with a 250 kN load cell. The cross-head speed was of  $16.7 \cdot 10^{-3} \text{ mm} \cdot \text{s}^{-1}$ . Room temperature tensile properties were determined according to the UNI EN ISO 6892-1:2016 specification.

Vickers microhardness tests (HV) were performed with a Leica VMHT micro Vickers tester (Leica Microsystems, Buccinasco (MI), Italy) with a load of 0.1 N and a dwell time of 15 s, in accordance with the UNI EN ISO 6507:2006 specification with the aim of testing the sole aluminum matrix.

### 2.3. Microstructural Investigations

Samples for microstructural investigations were cut from the tensile specimens, embedded in phenolic resin and prepared using standard grinding and polishing procedures. Microstructure analyses were performed using a Leica DMI8 polarized light optical microscope (OM, Leica Microsystems, Buccinasco (MI), Italy). In order to enhance the contrast between the Mg-based intermetallic and the Ni-based phases, the 0.5 mL HF + 100 mL H<sub>2</sub>O etchant was used. Quantitative

metallography was carried out using the LAS image analysis software. In accordance with the BS ISO 13322-1:2014, a measurement field was systematically defined over the six samples. Twenty frames, each having an area of  $\sim 10,600 \mu\text{m}^2$ , were analyzed at a magnification of  $1000\times$ . The total investigated area was thus of  $\sim 212,000 \mu\text{m}^2$ . Two different dedicated thresholds were set for eutectic Si particles and Ni-rich phases, respectively. Area fraction ( $A_f$  %), equivalent diameter ( $ED = (4A/\pi)^{1/2}$ ), and circularity ( $C = p^2/4\pi A$ ) [24] were selected as geometric parameters for this study. Statistical distribution fits of these parameters were evaluated with the Anderson-Darling (AD) test. Furthermore,  $A_f$  % uncertainty was estimated by encompassing two main contributions, one related to the operator and one to the instrument (constant value). An image generator software was used to create a reference image containing 20 different objects with known dimensions. The reference image was artificially blurred in order to reproduce the worst real case. Subsequently, the objects in the blurred image were measured 10 times. Objects were classified into four categories based on size. The operator uncertainty, with a level of confidence of approximately 95%, was assessed for each category as the standard deviation.

The different phases were also observed with a Zeiss EVO MA 15 scanning electron microscope (SEM, Carl Zeiss Microscopy, Milan (MI), Italy) and identified through energy dispersive X-ray spectroscopy (EDS, Oxford Instruments, Abingdon, Oxfordshire, United Kingdom). Deep-etched specimens were investigated to give a qualitative evaluation of the 3D structure of eutectic Si and Ni-containing compounds. According to [11] for the deep-etching analysis specimens were etched for a total time of 3 min, alternatively for 20 s in 10% NaOH and 5% HCl water solutions, respectively.

### 3. Results

#### 3.1. Mechanical Properties

##### 3.1.1. Tensile Properties

The results of tensile tests are depicted in Figure 1a,b for the as-cast and the T6 heat-treated alloys in terms of yield strength (YS) and ultimate tensile strength (UTS), respectively. Results for the A356 base alloy, without Ni additions, reported in a previous work [25], are also depicted with red markers in Figure 1a,b. It can be observed that in the as-cast condition the average value of YS increases from 74 MPa for the alloy with 0.5 wt % Ni to 83 MPa when the Ni concentration is 1 wt %. No further statistically significant variation is found by increasing the Ni content up to 2 wt %. Moreover, the UTS of the as-cast specimens does not appear to be dependent on the Ni concentration. On the contrary, in the T6 condition, a significant drop in mechanical properties can be observed as the Ni concentration reaches 2 wt % (YS: from 179 down to 110 MPa; UTS: from 287 down to 200 MPa). It is worth to point out that the mechanical properties of the heat-treated alloy with 2 wt % Ni are not so far from the values observed for the same alloy in the as-cast condition. Apparently, Ni seems to neutralize the positive effects of the T6 heat treatment to some extent.

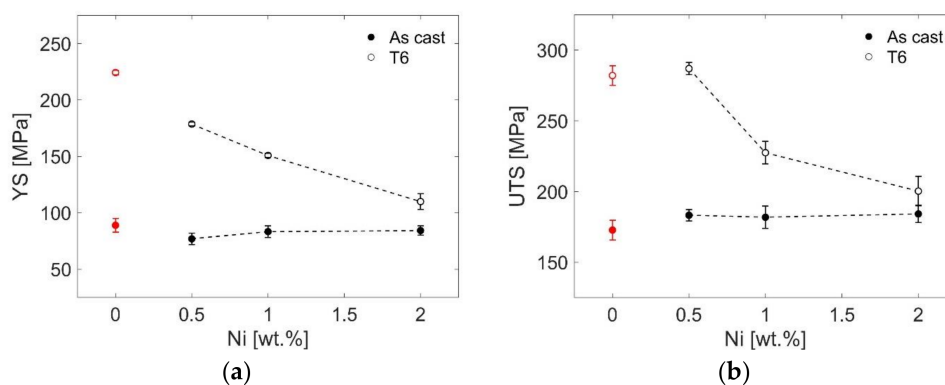


**Figure 1.** Tensile properties of specimens in as-cast and T6 conditions: (a) YS; (b) UTS. Red markers refer to the A356 base alloy, without Ni additions, as reported by Casari et al. [25].

### 3.1.2. Microhardness

Vickers microhardness measurements for the as-cast and the T6 conditions are reported in Figure 2 as a function of Ni content. Indentations were performed with a normal load of 0.1 N in order to evaluate the hardness of the sole primary Al matrix. As it can be observed, the microhardness remains constant as Ni increases for the as-cast specimens. After T6 heat treatment, as expected, microhardness values are higher. Nevertheless, a reduction of about 20 microhardness points between the lowest and the highest Ni content is noted.

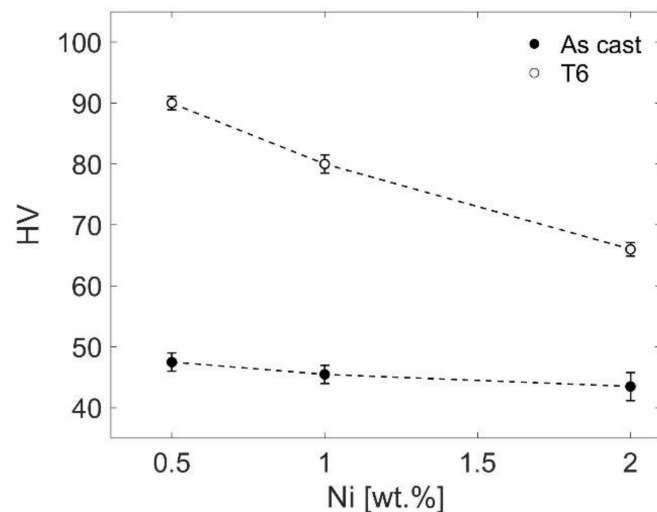


**Figure 2.** Vickers microhardness, with a normal load of 0.1 N, for as-cast and T6 heat-treated specimens.

## 3.2. Microstructural and Fractographic Observations

### 3.2.1. Microstructural Investigations

Representative SEM micrographs of the investigated alloys in the as-cast and T6 heat-treated conditions are depicted in Figure 3a–f, respectively, for 0.5, 1, and 2 wt % Ni. The typical microstructure of an A356 alloy can be observed, consisting of primary Al dendrites and eutectic Si particles in the interdendritic regions. Ni-bearing compounds can also be detected, with the number and size of such intermetallic compounds depending on the alloy chemical composition. These intermetallic compounds are observed primarily with a Chinese-script morphology; occasionally, a blocky polyhedral morphology can also be detected. These particles were identified as  $\epsilon$ -Al<sub>3</sub>Ni and T-Al<sub>9</sub>FeNi intermetallic compounds by means of EDS spectra and they are labeled in the microstructures of Figure 3. It is noteworthy to observe that  $\beta$ -Al<sub>5</sub>FeSi compounds were not detected in the investigated alloys. This is an expected result since for all the alloys the Ni/Fe ratio is always higher than 2 and, thus, it suggests that the total amount of Fe is bound to Ni in the T-Al<sub>9</sub>FeNi phase, as reported by Farkoosh et al. [13]. The application of the T6 heat treatment causes some changes in the microstructure: eutectic Si particles, with a needle-like morphology in the as-cast microstructure, become fine and fibrous after T6 heat treatment. A variation in the shape of particles can also be observed for the Ni-based intermetallic phases, which show rounded and smoothed edges.

Deep-etched specimens were observed by SEM in order to identify the 3D network formed by eutectic Si and Ni-rich intermetallic compounds. Figure 4a shows some intermetallic compounds found in the as-cast alloy with 1 wt % Ni (bright in the backscattered electron image, Figure 4b). The EDS analysis confirmed the presence of both T-Al<sub>9</sub>FeNi and  $\epsilon$ -Al<sub>3</sub>Ni, as indicated in the spectra of Figure 4c,d. Ni-based compounds show irregular and complicated 3D shapes connected one to another by eutectic Si plate-like particles.

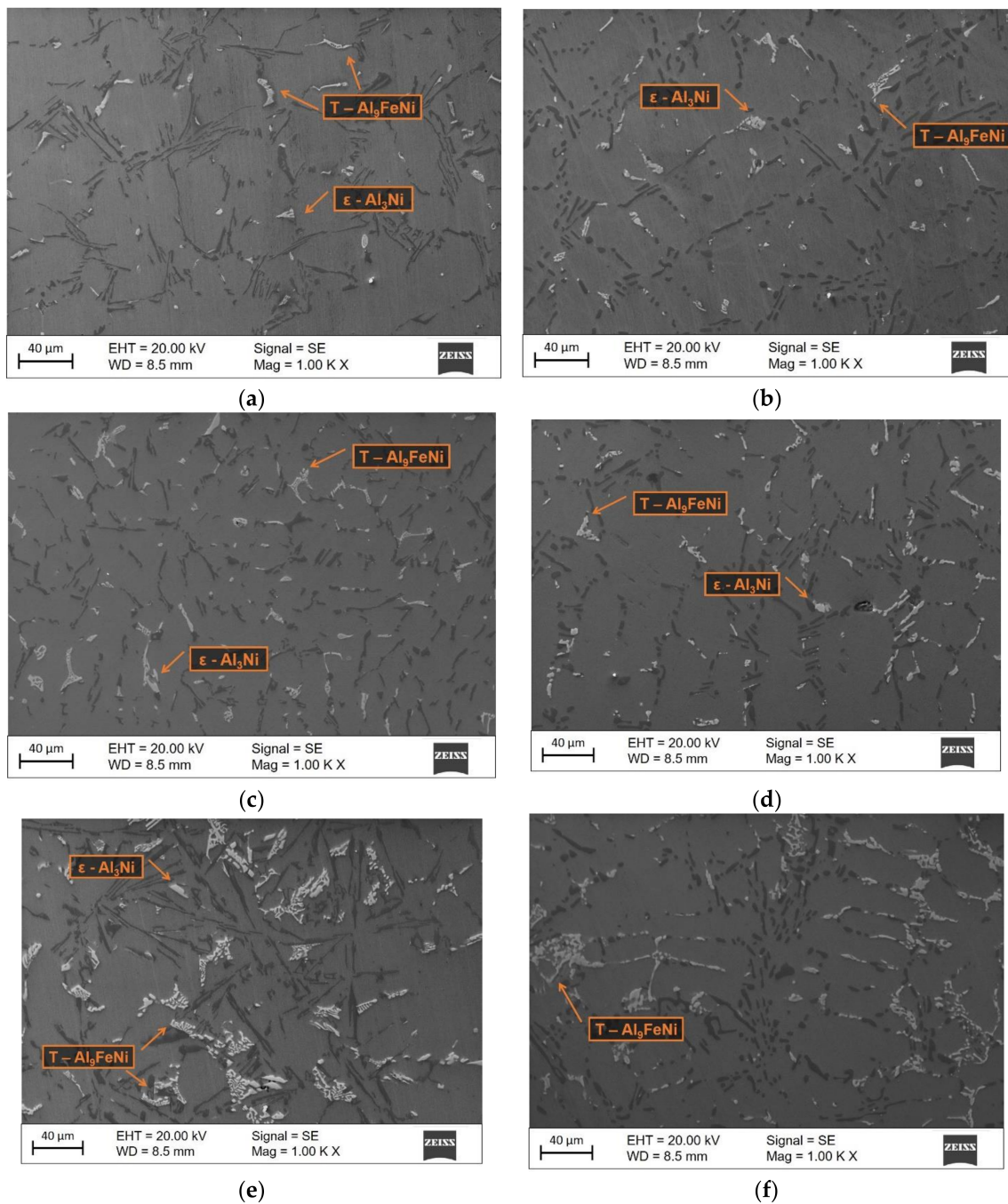


**Figure 3.** SEM micrographs (secondary electron images) of the alloys containing 0.5 (a,b); 1 (c,d) and 2 wt % Ni (e,f): (a,c,e) as-cast condition; and (b,d,f) T6 condition.

### 3.2.2. Fractography

Figure 5a–f illustrate the fracture surfaces of the alloys containing 0.5, 1, and 2 wt % Ni in the as-cast and heat-treated conditions. Figure 5a–f are SEM images acquired in backscattered electron mode in order to identify Ni-based compounds and eutectic Si. Extended cleavage regions can be easily distinguished within the as-cast samples. The presence of a large number of brittle phases on the fracture surface suggests that the crack originates and then propagates by rupture of such constituents, i.e., eutectic Si or Ni-based phases. After T6 heat treatment, plastic deformation regions can also be easily detected on the fracture surface. These regions appear less frequently on the fracture surfaces with Ni concentration increasing from 0.5 to 2 wt %.

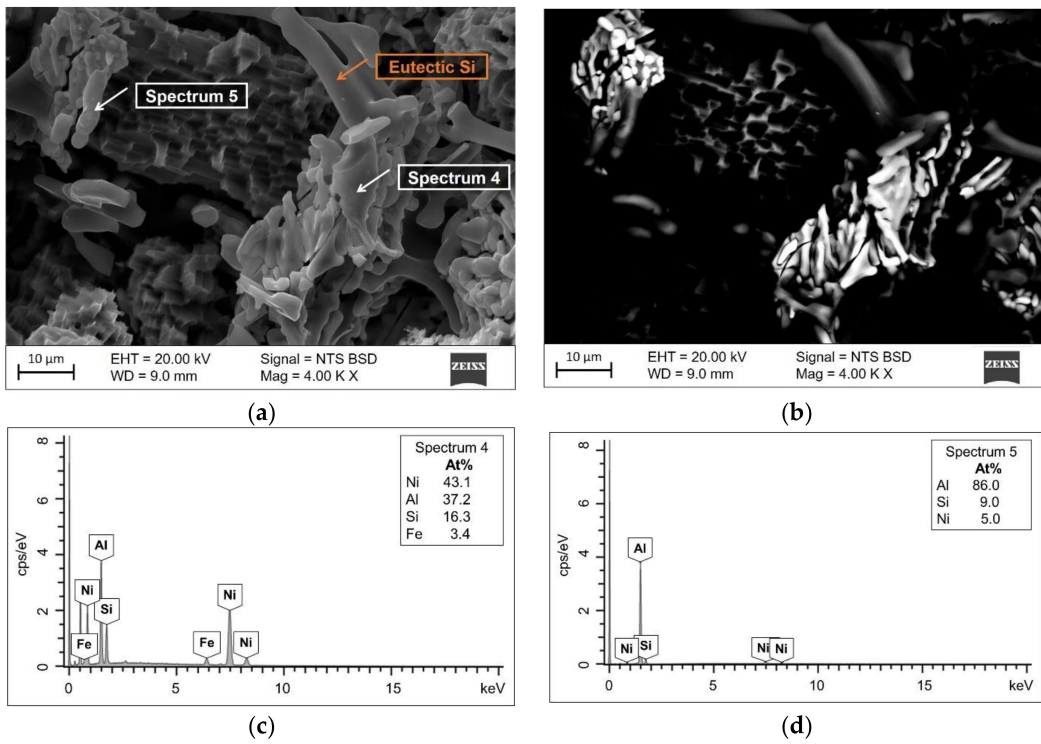


**Figure 4.** SEM micrographs of Ni-based intermetallic compounds in the as-cast alloy containing 1 wt % Ni: (a) secondary electrons; (b) backscattered electrons; EDS spectra: (c) T-Al<sub>9</sub>FeNi; and (d) ε-Al<sub>3</sub>Ni.

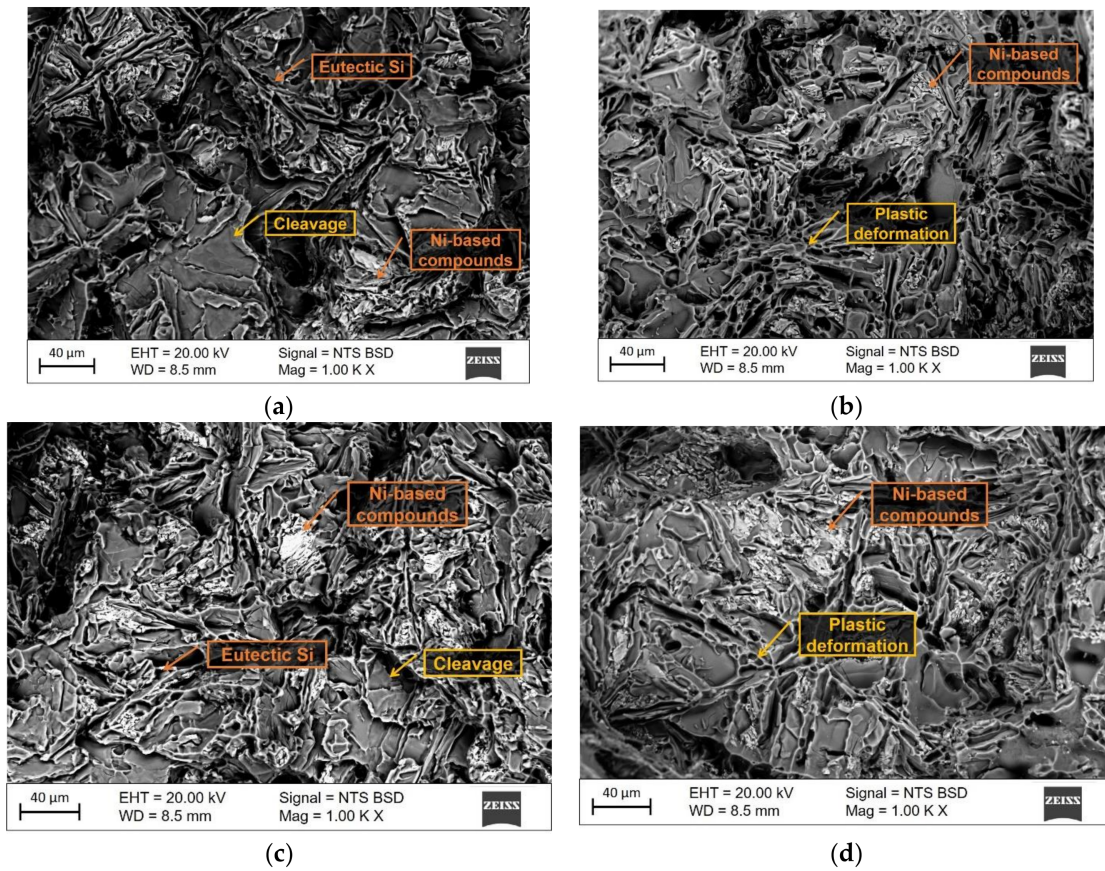


**Figure 5.** Cont.

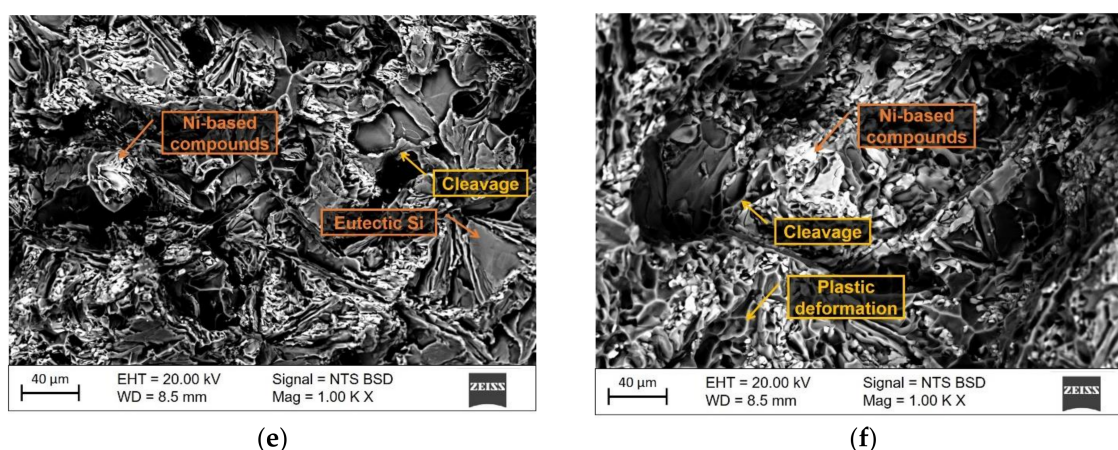


**Figure 5.** Fracture surfaces (backscattered electron images) of the alloys containing 0.5 (a,b); 1 (c,d) and 2 (e,f) wt % Ni: (a,c,e) as-cast condition; and (b,d,f) T6 condition.

### 3.3. Image Analysis and Statistical Evaluations

#### 3.3.1. Eutectic Si

A statistical evaluation of geometrical parameters after T6 heat treatment was performed for eutectic Si particles for all the investigated alloys. In light of the results found in the literature concerning the distribution of some geometrical parameters of eutectic Si particles [26,27], ED and C distributions were fitted with a three-parameter lognormal distribution and the goodness-of-fit was evaluated with the Anderson-Darling test. In particular, the closer the AD value is to 0, the better the fitting of data by a three-parameter lognormal distribution. Lognormal probability distribution parameters, scale  $\sigma$ , location  $\mu$ , and threshold  $\tau$  are listed in Table 2 along with AD statistics and mode values for ED and C of each investigated alloy in the T6 heat-treated condition. These findings are in agreement with the fact that geometrical parameters of eutectic Si particles follow a three-parameter lognormal distribution, as reported in the literature [26,27].

**Table 2.** Lognormal parameters for ED and C of Si eutectic particles in the investigated alloys, after T6 heat treatment.

Geometrical Parameter	Ni (wt %)	$\mu$	$\sigma$	$\tau$	AD	Mode
ED ( $\mu\text{m}$ )	0.5	1.537	0.39339	−0.679	0.50	3.31
	1	1.682	0.43720	−0.560	0.41	3.88
	2	1.506	0.52589	−0.057	0.27	3.36
C	0.5	−0.860	1.194	1.178	1.56	1.18
	1	−0.479	1.107	1.025	0.82	1.27
	2	−0.472	1.247	1.103	0.47	1.23

The probability density functions (PDF) for ED and C are depicted in Figure 6a,b, respectively. ED mode value increases from 3.31 to 3.88  $\mu\text{m}$  going from 0.5 to 1 wt % of Ni. It then slightly decreases to 3.36  $\mu\text{m}$  for 2 wt % of Ni. The peak height is higher for the alloy with 0.5 wt % of Ni, and it decreases for higher Ni contents. For what concerns C, similar observations can be made: its mode value is 1.18  $\mu\text{m}$  for 0.5 wt % of Ni and slightly increases to 1.27  $\mu\text{m}$  when the Ni content is 1 wt %. For 2 wt % of Ni, the C mode value reaches 1.23  $\mu\text{m}$ . The C variation with Ni content is very limited.

#### 3.3.2. Ni-Based Phases

With the aim of evaluating the influence of both Ni content and heat treatment on the morphology of Ni-based compounds, and thus their effect on alloy mechanical properties, ED and



C were investigated for such intermetallic compounds. ED and C distributions were fitted with a three-parameter lognormal distribution (Figure 7a–d) and the goodness-of-fit was evaluated with the AD test. Distribution parameters for ED and C of each investigated alloy are listed in Table 3 along with AD statistics and mode values. Despite some AD values being quite higher than others, it is worth noticing that the three-parameter lognormal distribution is the one with the lowest AD value for all the investigated alloys.

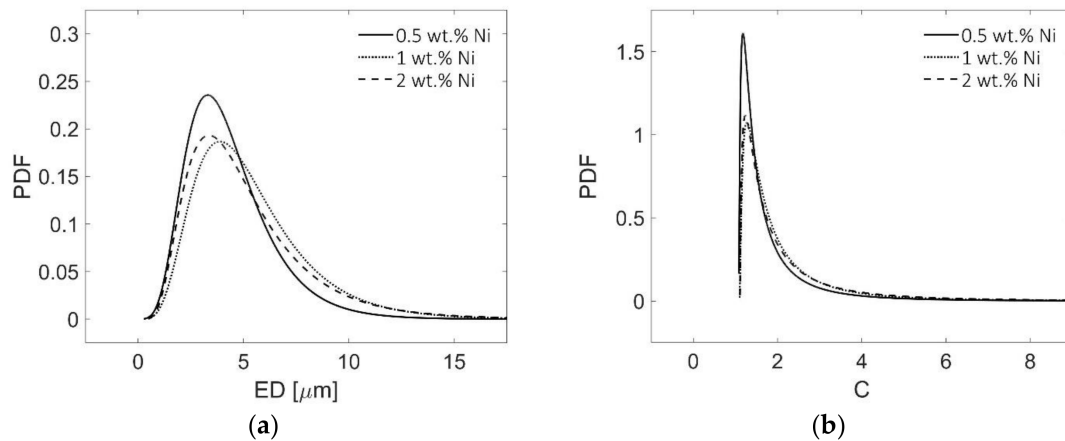


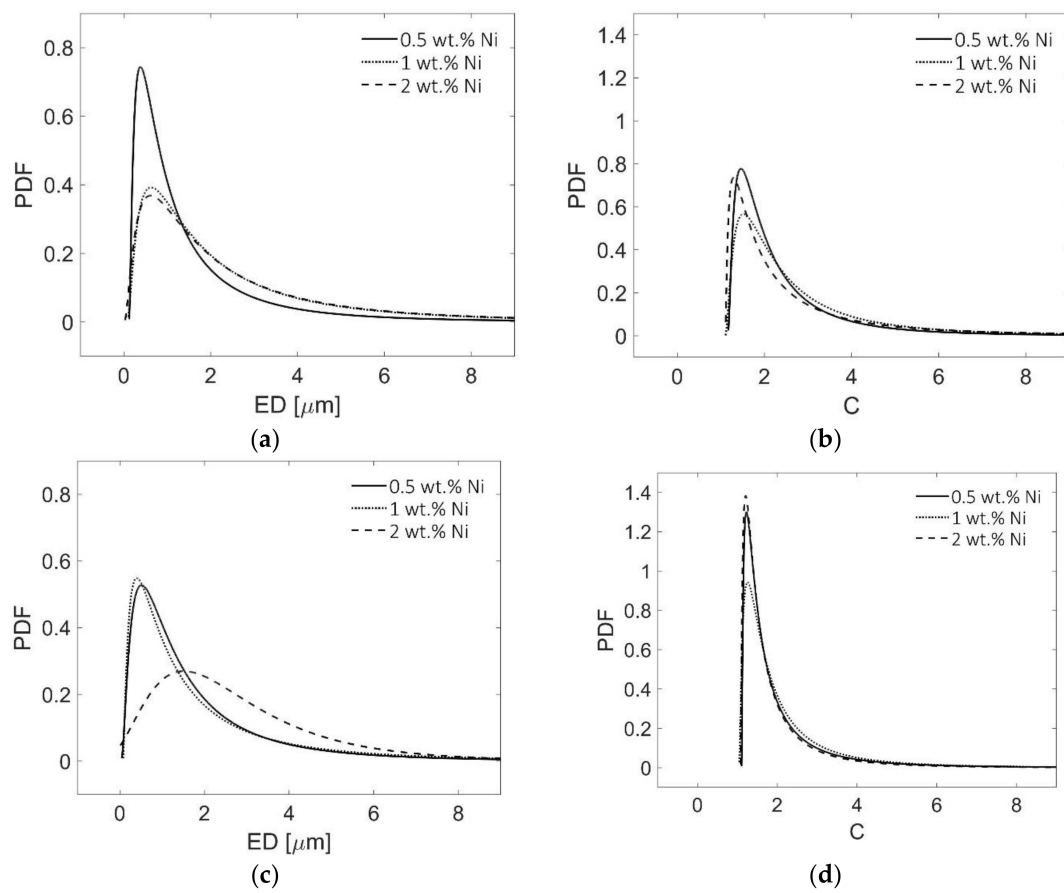
Figure 6. PDF for parameters of eutectic Si particles: (a) ED; and (b) C.

Table 3. Parameters of the lognormal distributions for ED and C of Ni-based intermetallic compounds for the three investigated alloys, in both as-cast and T6 conditions.

Geometrical Parameter	Condition	Ni (Wt %)	$\mu$	$\sigma$	$\tau$	AD	Mode
ED ( $\mu\text{m}$ )	As-cast	0.5	-0.114	1.098	0.115	1.93	0.38
		1	0.518	1.045	0.065	0.80	0.63
		2	0.579	1.027	-0.003	5.47	0.62
	T6	0.5	0.222	0.959	0.015	3.19	0.51
		1	0.199	1.133	0.065	3.16	0.40
		2	1.152	0.541	-0.849	2.59	1.51
C	As-cast	0.5	-0.167	1.002	1.152	0.23	1.46
		1	0.149	0.999	1.093	0.23	1.52
		2	-0.048	1.262	1.101	0.22	1.30
	T6	0.5	-0.643	1.204	1.104	1.14	1.23
		1	-0.354	1.081	1.038	1.99	1.26
		2	-0.724	1.147	1.077	0.65	1.21

In the alloy with the lowest Ni content compounds with an ED lower than 1  $\mu\text{m}$  are predominant. As expected, the size of Ni aluminides is found to increase as the content of Ni increases. Moreover, particles become more homogeneous in size as ED distribution peaks decrease and right tails increase. As can be noted in Figure 7c, after T6 heat treatment PDF values for ED decrease, meaning that the ED of Ni intermetallic compounds become more homogeneous. Turning now to the observation of C, it is important to underline that the C value approaches 1 when the particle shape is regularly round. Figure 7b highlights that in as-cast alloys particles show C modes between 1.30 and 1.52, while after T6 heat treatment (Figure 7d) C modes slightly decrease to an average value of 1.23.

Figure 8 shows the area fraction  $A_f$  % of Ni-rich phases as a function of Ni content, both in as-cast and T6 heat-treated conditions. In both cases,  $A_f$  % is found to increase as the Ni concentration increases. These results are in good agreement with the findings of Stadler et al. [6].



**Figure 7.** Distributions of geometrical parameters of Ni-based compounds: (a) ED, as-cast condition; (b) C, as-cast condition; (c) ED, T6 heat-treated condition; and (d) C, T6 heat-treated condition.

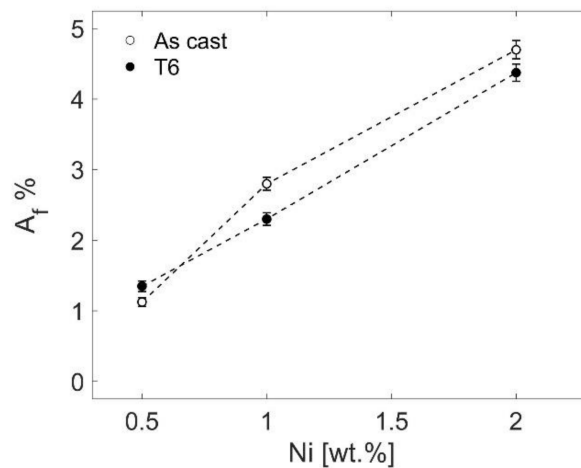


**Figure 8.** The  $A_f$  % of Ni-based compounds in as-cast and T6 heat-treated alloys as a function of Ni concentration.

## 4. Discussion

### 4.1. As-Cast Condition

In general, an Al-Si alloy can be considered as a composite material where the  $\alpha$ -Al phase is the matrix that needs to be reinforced, while the network of eutectic Si particles and Ni-based intermetallic compounds is the stronger phase acting as a reinforcement [9,10,16,21].

When an external load is applied, there is a non-uniform distribution of stresses due to the difference in elastic properties between the matrix and the reinforcing phases. In particular, when the rigid phase network is continuous and the matrix/reinforcement interface is extended, a load transfer occurs and a large part of the load is born by the rigid phase. Uggowitzner et al. [28] hypothesized that the continuity of the reinforcing phase is improved as its volume fraction increases, up to an upper limit above which there is no more improvement of the network continuity. The addition of increasing quantities of Ni to the A356 base alloy promotes the formation of Ni-based phases, thus increasing the volume fraction of the reinforcing phase. Nevertheless, the trend depicted in Figure 1a shows that YS remains almost constant, close to the value of the base A356 alloy, with increasing Ni content. This could be explained assuming that eutectic Si particles in the A356 alloy have already a good interconnectivity in the as-cast condition, as reported by Lasagni et al. [29]. For this reason, further additions of Ni do not determine an appreciable improvement in the bearing capability of the rigid reinforcing phase.

Similarly, the UTS remains constant as the Ni concentration in the alloy increases. It is, thus, clear that the formation of a larger amount of Ni aluminides does not exert any beneficial effect on the interconnectivity of the 3D network. On the contrary, the phases forming the reinforcing network have a similar tendency to initiate and propagate fracture [25,30]. These considerations seem to be consistent with fracture surface observations. Extended cleavage regions can be easily noticed on the fracture surfaces of as-cast alloys (Figures 4 and 5). The presence of several brittle phases and the lack of plastic deformation suggest that cracks initiate in brittle constituents, i.e., eutectic Si- or Ni-based intermetallic compounds, and easily propagate by cleavage of fragile phases or following the matrix/reinforcement interface. Furthermore, it is worth noting that eutectic Si particles, in the as-cast condition, show a plate-like morphology that could easily originate a localized stress concentration region.

ED of Ni aluminides increases, in the as-cast condition, when Ni content increases from 0.5 to 2 wt % (Figure 7a). The rising dimension of Ni-based compounds could suggest an enhanced interconnectivity of the reinforcing network, thus improving the tensile properties. Nevertheless, as previously mentioned, these hypotheses are not supported by the results of tensile tests. For what concerns *C*, the majority of its values ranges from 1 to 3 for each Ni content, hence, Ni particles show a similar morphology for the three investigated alloys. These findings suggest that the potential stress concentration near intermetallic compounds is similar and, thus, that their detrimental influence on tensile properties is negligible, which also justifies the observed YS and UTS trends.

Overall, these results indicate that in the as-cast condition fracture propagates either by cleavage mechanism through brittle phases, i.e., eutectic Si particles and Ni-based compounds, or by debonding of brittle phases from the Al matrix. The formation of a 3D network composed of the two rigid phases is not sufficient to determine an increase of mechanical properties of the alloys at room temperature.

#### 4.2. T6 Heat-Treated Condition

Figure 1a,b show that Ni has a clear detrimental effect on both the YS and the UTS of T6 heat-treated alloys. The reason for this behavior can be explained by the composite material approach and the mechanism of load transfer from the primary Al matrix to the reinforcement phases, suggested by Moffat [30] and re-proposed by Casari et al. [25]. This approach takes into account the empirical relation between hardness (*H*) and ultimate tensile strength (*UTS*), reported in Equation (1):

$$H = f(UTS) \quad (1)$$

In addition, it assumes that rigid phases, i.e., eutectic silicon particles and Ni-bearing phases, have a linear elastic behavior, thus the deformation of fracture  $\varepsilon_{fr}$  can be expressed by Equation (2):

$$\varepsilon_{fr} = f(UTS)/E \quad (2)$$

where  $E$  is Young's modulus, in GPa. Since an absolute relationship is not required, relative fracture strain  $f(\varepsilon_{fr})$  can be obtained by Equation (3), combining Equations (1) and (2):

$$f(\varepsilon_{fr}) = H/E \quad (3)$$

Assuming homogeneity of the strain distribution for each phase, the values of  $H$  and  $E$ , found in literature and reported by Moffat [30] and Song et al. [31], can be used in Equation (3) to determine the values of  $f(\varepsilon_{fr})$ , reported in Table 4. It is worth noting that Ni-rich compounds show a lower value of relative fracture strain compared to eutectic Si particles and, thus, have a higher tendency to fracture.

**Table 4.** Hardness, Young's modulus, and relative fracture strain for eutectic Si and Ni-based phases [30].

Phase	Hardness [GPa]	Young's Modulus [GPa]	$f(\varepsilon_{fr})$
Eutectic Si	11.13	147.6	0.0754
T-Al <sub>9</sub> FeNi	7.71	161.5	0.0477
$\varepsilon$ -Al <sub>3</sub> Ni	7.73 [31]	141.2 [31]	0.0548

These findings suggest the following fracture mechanism of the material: when an external stress is applied, the load is mainly born by the reinforcing network of eutectic Si and Ni aluminides. These phases show the highest tendency to fracture [25], leading to the formation of micro-cracks in the material. The specimen, thus, reaches YS for lower stress values. Furthermore, since micro-cracks can easily propagate across brittle phases, the fracture rapidly propagates when there is a high interconnectivity of the reinforcing 3D network. This leads to the formation of extended de-cohesion regions that reduce the dimension of the resistant section. For this reason, UTS is reached at lower stress values.

In comparison with the mechanical properties of the heat-treated A356 base alloy (Figure 1a,b), the addition of 0.5 wt % Ni has a detrimental influence on the YS of the alloy, since it yields a decrease of about 40 MPa owing to the early fracture of brittle Ni-based compounds. Likewise, a further decrease of 100 MPa at Ni contents up to 2 wt % can be clearly related to the increased area fraction of such intermetallics (Figure 8).

As far as UTS is concerned, both the base A356 alloy and the alloy with 0.5 wt % Ni exhibit a similar value. Apparently, this Ni content does not enable to maintain the 3D network after T6 heat treatment. Such loss of interconnectivity limits the ease of crack propagation by involving the more ductile Al phase in the fracture process, reasonably explaining the higher UTS average value than those of the alloys with 1 and 2 wt % Ni. In contrast, higher Ni concentrations limit the fragmentation and spheroidization of eutectic Si particles during T6 heat treatment [9,10,16,21]. As a result, the 3D network maintains a higher level of interconnectivity, fostering crack propagation through a much easier path and, thus, leading to lower UTS values.

These hypotheses seem also in line with fractographic observations of alloys with Ni contents of 0.5, 1 and 2 wt % (Figure 5b,d,f, respectively). In Figure 5b, the heat-treated alloy with low Ni content presents not only a certain number of cleavage regions and fractured brittle phases (mainly eutectic Si particles) but also plastic deformation of the Al matrix. On the other hand, in Figure 5d,f, a lower amount of plastic deformation can be detected and it is possible to distinguish an increased number of either cleavage propagation or debonding sites.

It is worth noting that the morphology of brittle phases influences the mechanical properties of the investigated alloys. Statistical evaluations of geometrical parameters highlighted that the presence of Ni leads to a reduction of the spheroidizing effect of heat treatment on eutectic Si particles. ED and C increase with Ni contents of 1 and 2 wt % compared to the same parameters of the alloy with 0.5 wt % of Ni, as can be observed in Figure 6a,b. With 1 and 2 wt % of Ni, eutectic Si particles maintain an irregular morphology after heat treatment (Figure 6a), which eases the localized concentration of stresses. This then leads to crack formation at lower load values. Additionally, a higher average

dimension of eutectic Si particles (Figure 6b) indicates that the network fragmentation during heat treatment is limited when Ni contents are 1 and 2 wt %. Eutectic Si particles of considerable dimension promote fracture propagation once it is nucleated, explaining the decrease in YS and UTS average values depicted in Figure 1a,b.

Figure 2 shows the detrimental effect of Ni content on Vickers microhardness of the  $\alpha$ -Al matrix after T6 heat treatment. It is well-known that the T6 heat treatment leads to the precipitation of the M-Mg<sub>2</sub>Si phase in nanometric particles, which act as a reinforcement and increase the microhardness of the  $\alpha$ -Al matrix. Nevertheless, microhardness is found to decrease with further Ni additions up to 2 wt % (Figure 2). This result, in agreement with the outcome of tensile tests, may indicate that the presence of Ni exerts a negative effect on the precipitation of reinforcing intermetallic compounds to some extent.

In summary, Ni aluminides cause a remarkable decrease in the room temperature YS, UTS, and Vickers microhardness of the A356 heat-treated alloy. Despite additions of Ni up to 2 wt % hindering spheroidization effects of eutectic Si particles during T6 heat treatment, they also promote the formation of a higher number of brittle phases that easily promote fracture propagation.

## 5. Conclusions

The effect of Ni additions up to 2 wt % on the room temperature tensile properties and Vickers microhardness of the A356 aluminum casting alloy has been investigated in this research paper. As-cast specimens show a constant trend for both YS and UTS with increasing Ni content, and a similar trend is also observed for the microhardness. Fracture surface characteristics and geometric parameters of Ni-based compounds suggest that fractures propagate either by cleavage through brittle phases or by debonding of such phases from the  $\alpha$ -Al matrix. The 3D network composed of eutectic Si particles and Ni aluminides seems to be insufficient to determine an increase of the mechanical properties of the alloys.

After T6 heat treatment, both tensile properties and microhardness exhibit a substantial decrease with increasing Ni content. The analysis of geometrical parameters related to eutectic Si particles show a fair increase in ED and C, suggesting a lower efficiency of the T6 heat treatment in the fragmentation of the 3D network. These findings are consistent with the fracture surface observations, where a transition in the fracture mechanism can be clearly distinguished as the concentration of Ni increases. Particularly, while the fracture mechanism involves both cleavage and debonding of brittle phases and plastic deformation of the  $\alpha$ -Al matrix in the alloy with 0.5 wt % Ni, the crack propagation is characterized almost totally by cleavage and debonding at a Ni concentration up to 2 wt %.

**Acknowledgments:** The authors would express their gratitude to Federico Poli, for his collaboration during melt preparation and specimen casting, and Enrico Maggiolini, for his assistance during tensile tests.

**Author Contributions:** M.T.D.G. and A.F. gave a substantial contribution to the conception of the work; they also performed the image analysis, hardness, and tensile tests. L.L. and M.G. analyzed data and wrote the paper. D.C. and M.D.S. performed the melt preparation and specimen casting and revised the work; and M.M., G.L.G., and E.C. coordinated the research as principal investigators. All the authors approved the content of the manuscript.

**Conflicts of Interest:** The authors declare no conflict of interest.

## References

1. Quested, T.E. Understanding mechanisms of grain refinement of aluminium alloys by inoculation. *Mater. Sci. Technol.* **2004**, *20*, 1357–1369. [[CrossRef](#)]
2. Darlapudi, A.; McDonald, S.D.; StJohn, D.H. The influence of Cu, Mg and Ni on the solidification and microstructure of Al-Si alloys. *IOP Conf. Ser. Mater. Sci. Eng.* **2016**, *117*, 1–7. [[CrossRef](#)]
3. Tocci, M.; Pola, A.; Raza, L.; Armellini, L.; Afeltra, U. Optimization of heat treatment parameters for a non-conventional Al-Si-Mg alloy with Cr addition by DoE method. *La Metall. Ital.* **2016**, *6*, 141–144.

4. Pola, A.; Montesano, L.; Tocci, M.; La Vecchia, G.M. Influence of ultrasound treatment on cavitation erosion resistance of AlSi7 alloy. *Materials* **2017**, *10*, 256. [[CrossRef](#)] [[PubMed](#)]
5. Asghar, Z.; Requena, G.; Zahid, G.H.; Rafi-ud-Din. Effect of thermally stable Cu- and Mg-rich aluminides on the high-temperature strength of an AlSi12CuMgNi alloy. *Mater. Charact.* **2014**, *88*, 80–85. [[CrossRef](#)]
6. Stadler, F.; Antrekowitsch, H.; Fragner, W.; Kaufmann, H.; Uggowitzer, P.J. Effect of main alloying elements on strength of Al-Si foundry alloys at elevated temperatures. *Int. J. Cast Met. Res.* **2012**, *25*, 215–224. [[CrossRef](#)]
7. Casari, D.; Poli, F.; Merlin, M.; Di Giovanni, M.T.; Li, Y.; Di Sabatino, M. Effect of Ni additions on A356 alloy's microstructure and high-temperature mechanical properties. *La Metall. Ital.* **2016**, *6*, 37–40.
8. Moffat, A.J.; Mellor, B.G.; Sinclair, I.; Reed, P.A.S. The mechanisms of long fatigue crack growth behavior in Al-Si casting alloys at room and elevated temperature. *Mater. Sci. Technol.* **2007**, *23*, 1396–1401. [[CrossRef](#)]
9. Asghar, Z.; Requena, G.; Boller, E. Three-dimensional rigid multiphase networks providing high-temperature strength to cast AlSi10Cu5Ni1-2 piston alloys. *Acta Mater.* **2011**, *59*, 6420–6432. [[CrossRef](#)] [[PubMed](#)]
10. Asghar, Z.; Requena, G.; Degischer, H.P.; Cloetens, P. Three-dimensional study of Ni aluminides in an AlSi12 alloy by means of light optical and synchrotron microtomography. *Acta Mater.* **2009**, *57*, 4125–4132. [[CrossRef](#)]
11. Rohatgi, P.K.; Sharma, R.C.; Prabhakar, K.V. Microstructure and mechanical properties of unidirectionally solidified Al-Si-Ni ternary eutectic. *Metall. Trans. A* **1975**, *6*, 569–575. [[CrossRef](#)]
12. Sreeja Kumari, S.S.; Pillai, R.M.; Pai, B.C. A study on the structural, age hardening and mechanical characteristics of Mn and Ca added Al-7Si-0.3Mg-0.6Fe alloy. *J. Alloys Compd.* **2008**, *453*, 167–173. [[CrossRef](#)]
13. Farkoosh, A.R.; Javidani, M.; Hoseini, M.; Larouche, D.; Pekguleryuz, M. Phase formation in as-solidified and heat-treated Al-Si-Cu-Mg-Ni alloys: Thermodynamic assessment and experimental investigation for alloy design. *J. Alloys Compd.* **2013**, *551*, 596–606. [[CrossRef](#)]
14. Belov, N.A.; Eskin, D.G.; Aksenov, A.A. *Multicomponent Phase Diagrams: Applications for Commercial Aluminum Alloys*; Elsevier Science: Oxford, UK, 2005; p. 233, ISBN 9780080456966.
15. Chen, C.-L.; Richter, A.; Thomson, R.C. Investigation of mechanical properties of intermetallic phases in multi-component Al-Si alloys using hot-stage nanoindentation. *Intermetallics* **2010**, *18*, 499–508. [[CrossRef](#)]
16. Asghar, Z.; Requena, G.; Kubel, F. The role of Ni and Fe aluminides on the elevated temperature strength of an AlSi12 alloy. *Mater. Sci. Eng. A* **2010**, *527*, 5691–5698. [[CrossRef](#)]
17. Mohamed, M.J.S. Influence of nickel addition effect of heat treatment on aluminum-silicon piston alloys. *Int. J. Sci. Res.* **2015**, *4*, 781–784.
18. Nwankwo, N.E.; Nwoke, V.U.; Nnuka, E.E. Effect of Ni-additions on the microstructure and mechanical properties of Fe-based chill-cast Al-Si alloys for production of pistons for automobile engine applications. *Int. J. Sci. Res. Eng. Technol.* **2015**, *1*, 21–24.
19. Yang, Y.; Yu, K.; Li, Y.; Zhao, D.; Liu, X. Evolution of nickel-rich phases in Al-Si-Cu-Ni-Mg piston alloys with different Cu additions. *Mater. Des.* **2012**, *33*, 220–225. [[CrossRef](#)]
20. Yang, H.; Watson, D.; Wang, Y.; Ji, S. Effect of Nickel on the Microstructure and Mechanical Property of Die-cast Al-Mg-Si-Mn Alloy. *J. Mater. Sci.* **2014**, *49*, 8412–8422. [[CrossRef](#)]
21. Stadler, F.; Antrekowitsch, H.; Fragner, W.; Kaufmann, H.; Uggowitzer, P.J. The effect of Ni on the high-temperature strength of Al-Si cast alloys. *Mater. Sci. Forum* **2011**, *690*, 274–277. [[CrossRef](#)]
22. Fang, L.; Zhang, X.; Hu, H.; Nie, X.; Tjong, J. Microstructure and tensile properties of squeeze cast aluminum alloy A380 containing Ni and Sr addition. *Adv. Mater. Proc. Technol.* **2017**, *3*, 362–373. [[CrossRef](#)]
23. García-Hinojosa, J.A.; González, C.R.; González, G.M.; Houbaert, Y. Structure and properties of Al-7Si-Ni and Al-7Si-Cu cast alloys nonmodified and modified with Sr. *J. Mater. Process. Technol.* **2003**, *143*, 306–310. [[CrossRef](#)]
24. Friel, J. *Practical Guide to Image Analysis*; ASM International: Materials Park, OH, USA, 2000; p. 158, ISBN 0871706881.
25. Casari, D.; Ludwig, T.H.; Merlin, M.; Arnberg, L.; Garagnani, G.L. The effect of Ni and V trace elements on the mechanical properties of A356 aluminium foundry alloy in as-cast and T6 heat-treated conditions. *Mater. Sci. Eng. A* **2014**, *610*, 414–426. [[CrossRef](#)]
26. Alexopoulos, N.D.; Tiryakioglu, M.; Vasilakos, A.N.; Kourkoulis, S.K. The effect of Cu, Ag, Sm and Sr additions on the statistical distributions of Si particles and tensile properties in A357-T6 alloy castings. *Mater. Sci. Eng. A* **2014**, *604*, 40–45. [[CrossRef](#)]

27. Tiryakioglu, M. Si particle size and aspect ratio distributions in an Al-7%Si-0.6%Mg alloy during solution treatment. *Mater. Sci. Eng. A* **2008**, *473*, 1–6. [[CrossRef](#)]
28. Uggowitzer, P.J.; Stüwe, H.P. Plasticity of ferritic-martensitic two-phase steels. *Z. Metallk.* **1982**, *73*, 277–285.
29. Lasagni, F.; Lasagni, A.; Marks, E.; Holapfel, C.; Muckich, F.; Degischer, H.P. Three-dimensional characterization of ‘as-cast’ and solution-treated AlSi12(Sr) alloys by high-resolution FIB tomography. *Acta Mater.* **2007**, *55*, 3875–3882. [[CrossRef](#)]
30. Moffat, A.J. Micromechanistic Analysis of Fatigue in Aluminium Silicon Casting Alloys. Ph.D. Thesis, University of Southampton, Southampton, UK, 2007.
31. Song, J.-M.; Lin, T.-Y.; Chuang, H.-Y. Microstructural characteristics and vibration fracture properties of Al-g-Si alloys with excess Cu and Ni. *Mater. Trans.* **2007**, *48*, 854–859. [[CrossRef](#)]



© 2018 by the authors. Licensee MDPI, Basel, Switzerland. This article is an open access article distributed under the terms and conditions of the Creative Commons Attribution (CC BY) license (<http://creativecommons.org/licenses/by/4.0/>).